Regular article

On the electrostatic potential assisted nucleation and growth of precipitates in Al-Cu alloy

Shang Fu [a], Huiqun Liu [a], Ning Qi [b], Bin Wang [a], Yong Jiang [a], Zhiquan Chen [b,*], Tao Hu [a,*], Danqing Yi [a,*]

[a] School of Materials Science and Engineering, Central South University, Changsha, Hunan 410083, China
[b] School of Physics and Technology, Wuhan University, Wuhan, Hubei 430072, China

ARTICLE INFO

ABSTRACT

The effect of electrostatic potential (EP), specifically without current and Joule heating effect, on the precipitation in aluminum alloy during artificial aging (180 °C) was investigated via microhardness testing, transmission electron microscopy (TEM), positron annihilation spectroscopy (PAS), and measurements of vacancy formation enthalpy and vacancy migration enthalpy. The results elaborated that EP promoted the nucleation of solute clusters/GP zones in the early stage during aging. After extended aging, highly dense fine precipitates were retained in Al matrix leading to an improved strength. EP-assisted artificial aging provides a new pathway to tailor the precipitation behavior in Al alloys.

© 2018 Acta Materialia Inc. Published by Elsevier Ltd. All rights reserved.

Conventional precipitation-hardened Al-Cu-X series aluminum (Al) alloys have been widely used in aerospace and transportation industries due to their high specific strength and heat workability [1,2]. In this class of precipitation-hardened light alloys, extremely small and uniformly distributed Guinier-Preston (GP) zones and plate-shaped precipitates ($\theta'' + \theta'$), which act as obstacles to dislocation movement, form within the Al grain interiors upon thermal treatment and thus strengthen the material primarily. This phenomenon is generally referred as precipitation strengthening. It is generally accepted that the precipitation in Al-Cu alloys starts with the formation of solute clusters (1–2 nm), which sequentially evolved into GP zones → θ'' → θ' → θ phases [2–4]. A vast body of literature, published primarily in the last four decades, indicated that the formation of solute clusters/GP zones substantially depends on quenched-in vacancies in early stage of thermal treatment in precipitation-hardened Al alloys, specifically in Al-Cu, Al-Cu-Mg and Al-Mg-Si alloys [5–14]. Basically, the presence of high number density of GP zones and fine $\theta'' + \theta'$ phases is crucially responsible for the strengthening of the materials. In an effort to accelerate aging kinetics, artificial aging is usually performed. The commonly used artificial aging treatment for Al-Cu-Mg and Al-Cu-Li alloys is T8 temper which results in peak microhardness at 180 °C for 12 h.

To optimize the mechanical properties of precipitation-hardened Al alloys, the type and/or dispersion of the fine precipitates were usually tailored by applying external physical fields, e.g. stress field [15,16],

magnetic field [17,18], electric current field [19–21] and electric potential field [22–32], prior to/during artificial/natural aging treatment. The magnetic field and electric current field promoted the precipitation by enhancing the migration of solute atoms, while the stress field provided more nucleation sites and diffusion paths for precipitates via dislocations. Among them, electrostatic potential (EP)-assisted heat treatments, including sole EP effect [23,24,30–32], EP + current co-effect [26–28], resulted in changed precipitation behavior in Al alloys. In particular, the EP coupled thermal treatment induced early precipitation of β' and T1 phase in 6022 Al-Mg-Si alloy during natural aging [26] and in 2091 Al-Li alloy during artificial aging [29]. It increased the volume fraction of S′ or T1 phase at under-aged state in 2524 Al-Cu-Mg alloy [30] and Al-Cu-Li alloy [31], respectively. However, literature inspection indicated that how EP affects the nucleation or transition of meta-stable precipitates, how EP affects homogenization or aging treatment, has heretofore never been reported. Motivated by this lack of information, in this study, we investigated the effect of EP, specifically no electric current during aging treatment, on the nucleation and growth of fine precipitates (GP zones, θ'' and θ' phase) in an Al-Cu model alloy via two-step aging, microstructure characterization, positron annihilation spectroscopy (PAS) microhardness tests, measurement of enthalpy for vacancy formation and vacancy migration.

The raw material Al-4 wt%Cu (designated as Al-4Cu) in this work was prepared by casting in the lab. The measured composition of this alloy can be found in Supplementary Information (SI). The as-received samples were solution treated at 500 °C for 60 min and subsequently quenched into ice water. The as-quenched samples were divided into four groups and then subjected to different aging treatment routes.

Samples in Group A were aged at 180 °C for maximum 1320 min (22 h). Samples in Group B were aged at 180 °C for maximum 1320 min (22 h) with additional EP during the entire aging. Samples in Group C were aged at 180 °C for maximum 1320 min (22 h) with EP applied after 60 min (without EP in the first 60 min). Samples in Group D were aged at 180 °C for maximum 1320 min (22 h) with EP applied only in the first 60 min. The detailed sample information can be found in Table 1. The scheme of experimental setup is presented in Fig. S1 in SI. A positive EP of 5 kV was applied onto the sample. No current was detected during the entire aging excluding the Joule heating effect. The Vickers' hardness was measured on a HV-10B hardness tester with a load of 1500 g and a dwell time of 15 s by using a pyramid tip. The mean hardness ± standard deviation was obtained from at least 10 individual indentations. Positron annihilation spectroscopy (PAS) analysis were performed on a constant-fraction differential discriminator (ORTEC, US). The transferring of the aged specimens from the furnace to the discriminator was less than 5 min. Microstructure characterization was performed on a FEI Tecnai G2 20 TEM operated at 200 kV. Quantitative TEM analysis for the precipitates size was conducted by measuring 100 to 800 precipitates from 4 to 10 different areas of the TEM thin foil. To determine the vacancy formation enthalpy and vacancy migration enthalpy, various thermal treatment routes have been applied on pure Al specimens. The detailed method can be found in SI.

Fig. 1 shows the hardness vs. aging time curves of Al-4Cu alloy aged with or without EP assistance. The age-hardening curves for Samples A (without EP) and B (with EP) exhibit similar trend. However, due to the effect of EP, the overall hardness of Sample B is higher than that of Sample A before the peak-aging. The time for obtaining peak-aged hardness for Sample A and B is 960 min and 810 min, respectively. This indicated that EP shortens the time for achieving peak-aged hardness in Al-4Cu alloy during artificial aging. The hardness values of Sample C were almost as the same as those of Sample A in the first 60 min, in which no EP was applied. By applying EP after 60 min aging, however, the overall hardness of Sample C was lower than that of Sample A. The peak-aged stage with a relative low maximum hardness value of ~87 HV emerged around 810 min. The hardness values of Sample D were almost as the same as those of Sample B in the first 60 min, in which both have EP applied. The removal of EP after 60 min aging (in sample D) significantly facilitates the hardness increment. Moreover, the peak-aged stage for sample D appeared at 540 min, which is 270 min earlier than that for sample B and C. The peak-aged hardness of Sample D is ~115 HV, which is the highest value among four types of samples.

Fig. 2(a1) to (a3) show the microstructure of Al-4Cu alloy subjected to the aging at 180 °C without EP (Sample A). The aging treatment results in relatively low number density of precipitates in Al-4Cu alloy after 60 min while peak aging coarsens the precipitates. By applying EP during the entire aging as shown from Fig. 2(b1) to (b3), the number density of precipitates increased prominently after 60 min. Further extended aging to 120 min causes the growth/coarsening of the precipitates. However, at the peak-aging stage, the number density of the precipitates is higher than that of the sample A. To elucidate the effect of EP on early precipitation, EP was applied only after 60 min aging (Sample C). Fig. 2(c1) showed that, even aged with EP for the later 60 min, the size of the precipitates was close to that in samples aged without EP (Fig. 2(a2)). However, further aging with EP caused the growth/merging of the precipitates before/at peak-aging stage as
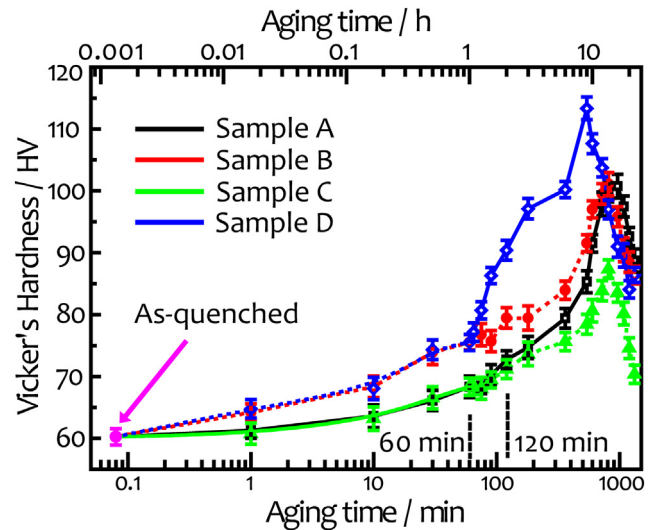
Table 1
Thermal treatments for Al-4Cu samples.

Sample ID	Thermal treatment routes
A	180 °C aging for maximum 1320 min
B	180 °C aging with EP for maximum 1320 min
C	180 °C aging for 60 min, then continue aging at 180 °C with EP
D	180 °C aging with EP for 60 min, then continue aging at 180 °C without EP

Fig. 1. The evolution of Vicker's hardness of Al-4Cu samples aged with/without EP for various durations.

shown in Fig. 2(c2). In contrast, when applying EP only in the first 60 min and removed EP then (Sample D), the high density of precipitates was reserved as shown in Fig. 2(d1) and (d2).

The SAED patterns indicated that the precipitates are primarily θ' phase (see Fig. S7 in SI), which may co-exist with θ'' phase. The size of the precipitates, particularly the length, was shown in Fig. 3. The length of the precipitates in Sample A after 60 min and 960 min (peak-aged stage) was 11.5 ± 2.5 nm and 50.5 ± 5.7 nm, respectively. Sample B was aged with EP throughout the entire thermal treatment. The length of the peak-aged sample B was determined as 46.2 ± 4.9 nm, which was very close to the value of 50.5 ± 5.7 nm in Sample A. After 120 min aging, the length of precipitates in Sample C was 11.6 ± 2.6 nm, which was similar to that in the Sample A aged for 120 min. Further extended aging from 120 min to peak-aged stage with EP, the length of the precipitates in Sample C was 87.6 ± 5.4 nm, which is more than that value of 50.5 ± 5.7 nm in the peak-aged Sample A. Sample D was initial aged with EP, and then continued aging without EP. After 120 min aging, the length of Sample D was measured as 6.9 nm ± 2.4 nm, which was relatively lower than that in Sample A, Sample B and Sample C. At subsequent aging, the length of the peak-aged Sample D was measured as 31.2 nm ± 5.9 nm, which was the lowest among all the four samples. It means that Sample D experienced a moderate coarsening at extended aging.

The thickness of TEM foils was determined by measuring the spacing of parallel Kossel–Mollenstedt fringes in a $\{020\}_{Al}$ reflection in a two-beam $\langle 001 \rangle_{Al}$ convergent beam electron diffraction pattern [33-35]. The detailed analysis of the precipitate number density and volume fraction were also listed in Table 2. The calculation of strength increment due to the precipitates can be found in SI. It showed that the strength increment from Orowan dislocation by-passing is the operative mechanism in this study. In addition, the strength increment follows the trend: $\Delta\sigma_{orowan}$ (Sample D) > $\Delta\sigma_{orowan}$ (Sample B) > $\Delta\sigma_{orowan}$ (Sample C) > $\Delta\sigma_{orowan}$ (Sample A) for all four samples after 120 min aging. Therefore, the highly dense precipitates in Sample B and Sample D caused by EP led to larger strength increment in the first 120 min. This interpretation agreed well with the aging hardening curves in Fig. 1.

Previous studies with primarily focus on applying electric field during homogenization indicated that EP with current on Al-Mg-Si-Cu alloy (AA6111) would increase the solubility of solute atoms via reducing the Gibbs free energy [28], whereas the sole EP effect retarded the peak-aging in 2091 Al-Li alloy [24] after homogenization and aging treatment both coupled with EP. However, our results